# PROCEEDINGS OF SPIE

SPIEDigitalLibrary.org/conference-proceedings-of-spie

Strain engineering photonic properties in monolayer semiconductors through mechanically-reconfigurable wrinkling

Hossain, M., Zhang, Yue, van der Zande, Arend

M. Abir Hossain, Yue Zhang, Arend M. van der Zande, "Strain engineering photonic properties in monolayer semiconductors through mechanically-reconfigurable wrinkling," Proc. SPIE 11464, Physical Chemistry of Semiconductor Materials and Interfaces XIX, 1146404 (20 August 2020); doi: 10.1117/12.2567539



Event: SPIE Nanoscience + Engineering, 2020, Online Only

# Strain engineering photonic properties in monolayer semiconductors through mechanically-reconfigurable wrinkling

M. Abir Hossain<sup>a</sup>, Yue Zhang<sup>a</sup>, and Arend M. van der Zande<sup>a,b</sup>

<sup>a</sup>Mechanical Science and Engineering, University of Illinois at Urbana-Champaign, 1206 W. Green St., Urbana, IL, USA

<sup>b</sup>Material Research Lab, University of Illinois at Urbana-Champaign, 104 S. Goodwin Ave., Urbana, IL, USA

### ABSTRACT

Inhomogeneous and three-dimensional strain engineering in two dimensional materials opens up new avenues to straintronic devices for control strain sensitive photonic properties. Here we present a method to tune strain by wrinkling monolayer WSe<sub>2</sub> attached to a 15 nm thick ALD support layer and compressing the heterostructure on a soft substrate. The ALD film stiffens the 2D material, enabling optically resolvable micron scale wrinkling rather than nanometer scale crumpling and folding. Using photoluminescence spectroscopy, we show the wrinkling introduces periodic modulation of the bandgap by 47 meV, corresponding with strain modulation from +0.67% tensile strain at the wrinkle crest to -0.31% compressive strain at the trough. Moreover, we show that cycling the substrate strain mechanically reconfigures the magnitude and direction of wrinkling and resulting band tuning. These results pave the way towards stretchable multifuctional devices based on strained 2D materials.

**Keywords:** 2D materials, Strain Engineering, Nanomechanics

# 1. INTRODUCTION

Strain engineering to tailor material properties is frequently used in technology, from enhancing the mobility and reducing inter valley scattering in silicon based transistors, to reducing hole effective mass in group iii-v semiconductor lasers.<sup>1,2</sup> Due to their atomic scale dimensions, 2D materials offer a new capability of easily achieving large and spatially inhomogeneous strains by inducing out-of-plane deformations.<sup>3,4</sup> In plane tensile strain strongly modulates the optical band gap of transition metal dichalcogenides (TMDs); most relevantly, under tensile strain, the optical band gap of WSe<sub>2</sub> decreases linearly by 48 meV/% strain,<sup>5</sup> with similar tuning in other 2D materials.<sup>6,7</sup> Furthermore, inducing large inhomogeneous strain gradients, either by nanoscale indentation or by transferring TMDC layers onto patterned substrates, leads to spatially inhomogeneous strain that locally modulates the band gap.<sup>8</sup> This inhomogeneous strain has applications such as isolated single quantum emitters and artificial atoms,<sup>9-12</sup> and combinations of directed exciton drift or conversion.<sup>13,14</sup>

In most of the previous studies, the strain profile of the 2D material is fixed, and the method of inducing the strain is not conducive to integrating into devices. Strategies from stretchable electronics<sup>15</sup> and crumpling of 2D materials point to an alternate strategy for engineering the strain through the controlled self assembly of 3D structures from thin films on compressed soft substrates. Because of the low bending modulus and adhesion of 2D materials, compression leads to crumpling behavior and buckle delamination. While crumpling has numerous applications in multifunctional surfaces and deformable devices,<sup>4,16,17</sup> it prevents large in-plane strains from building up in the material.<sup>18</sup> Larger strains may be achieved by interfacing the 2D material with a stiffer substrate. For example, few nanometer thick skin layers have recently been shown to lead to crack-free, micron scale wrinkling and efficient strain transfer in monolayer graphene.<sup>19–22</sup> Applying similar principles to other

Further author information: (Send correspondence to A.M.v.d.Z.)

A.M.v.d.Z.: E-mail: arendv@illinois.edu M.A.H.: E-mail: mah5@illinois.edu Y.Z.: E-mail: yuez11@illinois.edu

Physical Chemistry of Semiconductor Materials and Interfaces IX, edited by Christian Nielsen, Daniel Congreve, Andrew J. Musser, Proc. of SPIE Vol. 11464, 1146404 · © 2020 SPIE · CCC code: 0277-786X/20/\$21 · doi: 10.1117/12.2567539

2D materials will enable inhomogeneous strain and enable new classes of straintronic devices and access to new quantum states. Here, we demonstrate a simple method for mechanically reconfigurable and inhomogeneous strain engineering of photonic properties via wrinkling of monolayer TMDCs attached to a thin membrane of atomic layer deposition grown aluminum oxide on a soft, stretchable substrate.

### 2. FABRICATING WRINKLED 2D MATERIALS

Figure 1(a) shows the fabrication process flow to make the wrinkled heterostructures of monolayer WSe<sub>2</sub> on a 15 nm thick ALD Aluminum oxide, on a soft substrate made of very high bonding (VHB, 3M Inc.) tape. Figure 1(b)-(c) show optical image and Atomic Force Microscopy (AFM) topographic image of the resulting wrinkled structure at 10% compression.

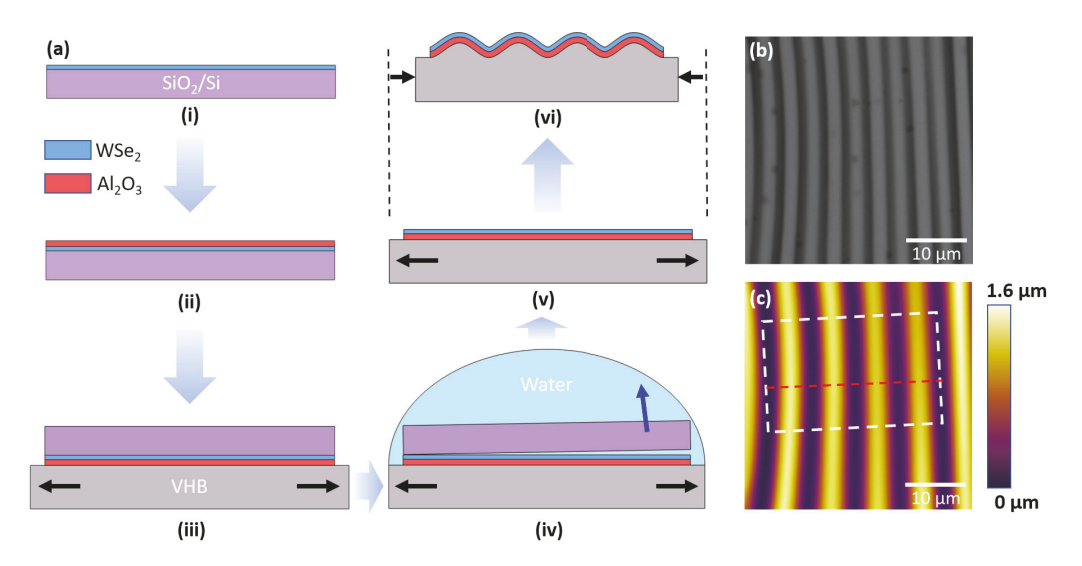


Figure 1. Uniaxially wrinkled  $WSe_2$ - $Al_2O_3$  heterostructure on a stretchable substrate. (a) Schematic illustration of the fabrication process flow of a wrinkled structure with individual steps described in the text. (b) Optical image of the resulting wrinkled heterostructure under 10% uniaxial compression. (c) Corresponding Atomic Force Microscopy (AFM) topographic map of the same region. The dashed white rectangle and red line represents the area used for photoluminescence mapping and cross-sectional profile, respectively.

Outlined in Figure 1(a), we fabricated the wrinkled architectures using the following procedure. (i) We used recently reported large area exfoliation techniques<sup>23</sup> to delaminate a monolayer using stamping of thin film gold onto bulk WSe<sub>2</sub> then transfer the gold/monolayer onto a 285 nm thick SiO<sub>2</sub> on silicon substrate. We used iodine/potassium iodide-based gold etchant to remove the gold, which leaves a continuous monolayer of WSe<sub>2</sub>, with lateral dimensions of 300  $\mu$ m to 1 mm, limited primarily by the size of the bulk crystal. The advantage of this technique over chemical vapor deposition (CVD) grown materials is the exfoliated material has much higher optical quality, and is more mechanically robust with much less cracking through the transfer and delamination procedures. (ii) We used Atomic Layer Deposition (ALD) to grow 15 nm thick Al<sub>2</sub>O<sub>3</sub> on top of the WSe<sub>2</sub> monolayer. (iii-v) We transferred the WSe<sub>2</sub>-Al<sub>2</sub>O<sub>3</sub> heterostructure on to a pre-strained VHB substrate. We adhere pre-strained VHB to the heterostructure on SiO<sub>2</sub>, then gently pull the substrates apart while immersed in DI water.<sup>24</sup> While the ALD film has very high adhesion to both the 2D material and the SiO<sub>2</sub>, the binding of the 2D material to the SiO<sub>2</sub> is low. As a result, the membrane tears along the edge of the 2D material, and all the region covered by 2D material is delaminated while the region with no 2D material is left on the SiO<sub>2</sub>. The end result is a flat membrane of monolayer WSe<sub>2</sub> on Al<sub>2</sub>O<sub>3</sub> on the pre-strained VHB substrate. (vi) As the final step, we released the pre-strain in the substrate by controlled percentages, inducing compression and wrinkles of the WSe<sub>2</sub> and ALD film. Initially, we start with prestrains of 10% or 25%. Shown in Figure 1(b-c) after releasing a pre-introduced strain of 10%, the surface buckles into a periodically wrinkled structure. The wavelength of the wrinkles is  $6.8 \pm 0.1 \mu m$ , and the amplitude is  $1.3 \pm 0.1 \mu m$ . This behavior is expected for stiff thin films under compression that are well adhered to a soft substrate.<sup>25,26</sup> We also tried similar experiments with PDMS but found that the lower adhesion strength lead to buckle delamination of the ALD films rather than uniform wrinkling. As a result of the large amplitude of wrinkling, the WSe<sub>2</sub> experiences periodic variation in strain on the surface of the ALD film.

### 3. INHOMOGENEOUS STRAIN ENGINEERING OF PHOTONIC PROPERTIES

In Figure 2, we use photoluminescence (PL) spectroscopy to visualize the strain-induced band-structure modification and resulting photonic properties caused by the wrinkling of the monolayer WSe<sub>2</sub>. Figure 2(a) shows the topography cross-section of the wrinkles. Figure 2(b),(c) show maps of the photoluminescence emission energy and intensity respectively, aligned to the corresponding topography profile. Figure 2(d) shows photoluminescence spectra of the monolayer WSe<sub>2</sub> at the crest and trough of a wrinkle, along with a spectra from a flat region on the same sample, which is similar to the spectra before compression. The spectra are captured in a Renishaw spectrometer with excitation wavelength of 532 nm, and the laser power of 31.6  $\mu$ W. Here we observe the optical transition energy and intensity are strongly modulated across the wrinkles, and remain constant along the wrinkles. For the flat region, the optical transition occurs at 1.64 eV, with a full width half max (FWHM) of 81 meV. After compression, the optical transition shifts by different amounts at different points along the wrinkle. The optical A-exciton transition shifts to 1.61 eV and 1.65 eV, corresponding to -32 meV redshift and +15 meV blueshift, at the crest and trough of a wrinkle, respectively. At the crest and trough of the wrinkled structure, the monolayer WSe<sub>2</sub>-Al<sub>2</sub>O<sub>3</sub> heterostructure goes through out of plane bending which introduces in plane tensile and compressive strain in the crest and trough, respectively. By comparing the energy shifts to previous measurements of uniformly strained WSe<sub>2</sub> and other 2D materials, <sup>5-7</sup> we estimate a uniaxial tensile strain of +0.67% at the wrinkle crest. While we could not find studies about tuning the band structure of WSe<sub>2</sub> under the uniaxial compression, assuming linear tuning at small compression yields a compressive strain of -0.31% at the trough. These strains are much smaller than the induced substrate compression of >10%. This is because wrinkling relaxes the overall strain from substrate compression. The effective straining of the 2D material is the much smaller residual strains on the surface of the wrinkles.

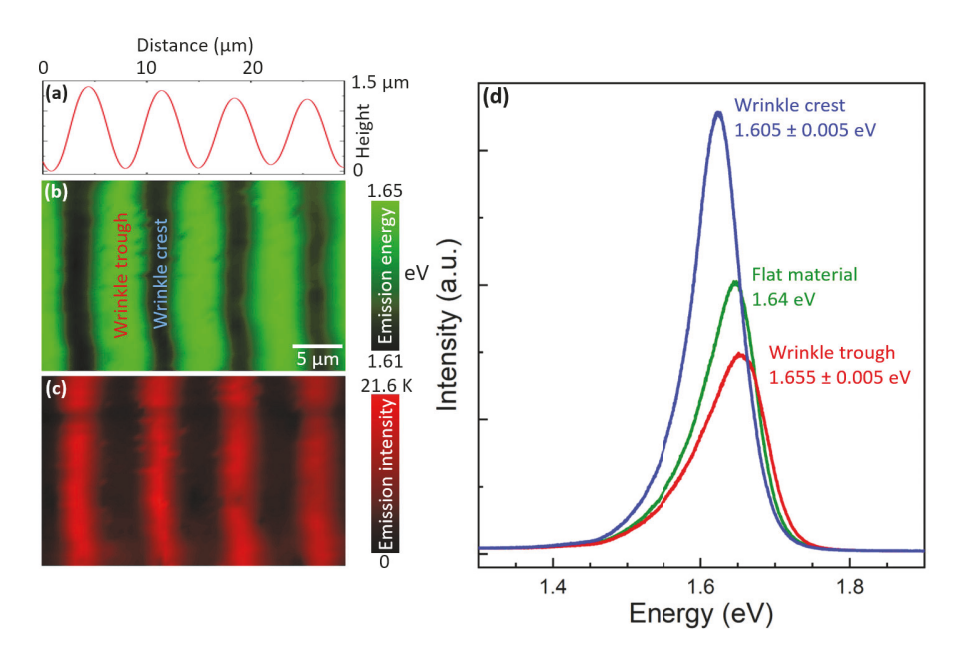


Figure 2. Mapping the photonic properties of the wrinkled monolayer WSe<sub>2</sub>. (a) AFM height measurement result along the red dashed line as shown in Fig 1 (b-c) Maps of the photoluminescence emission energy and intensity respectively for the region shown in 1, lined up with the corresponding topography. (d) Single photoluminescence spectra from the crest (blue) and trough (red) of the wrinkled WSe<sub>2</sub>. We compare the results to a spectra coming from a flat region (green), which is similar to the measured spectra before compression.

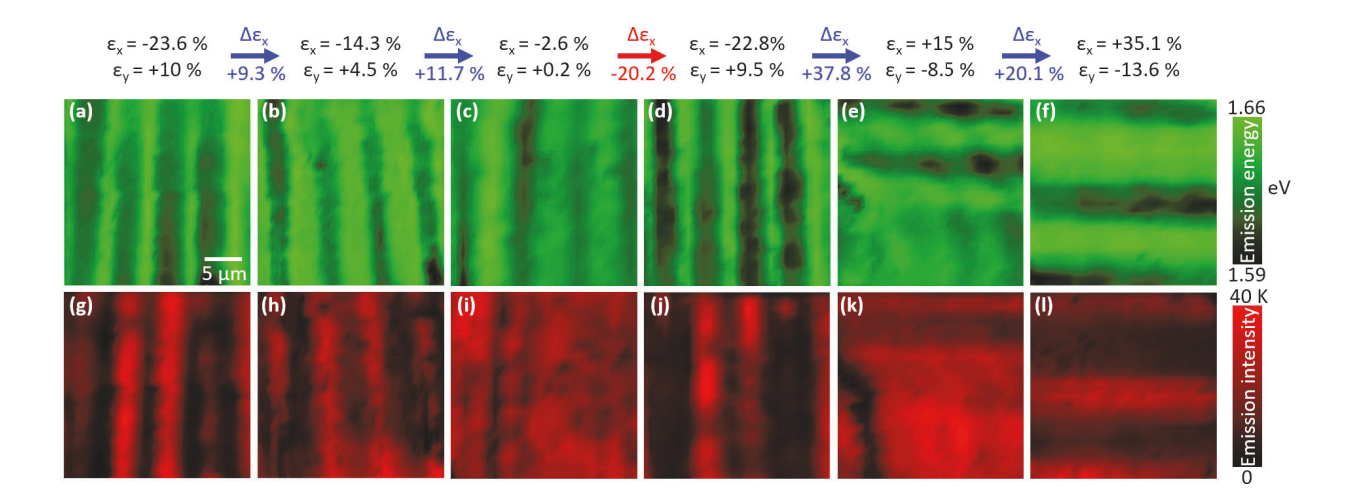


Figure 3. Evolution of the photoluminescence emission energy and intensity maps during the mechanical reconfiguration. The scan region is kept to  $25\mu m \times 25\mu m$ . (a)-(f) Photoluminescence transition energy maps (top), and (g)-(l) Photoluminescence intensity maps (bottom) under different strains levels. Strain levels are indicated at the top of each column. We use 532 nm excitation and laser power of 7.9  $\mu W$ .

As seen in Figure 2(c)-(d), there is also strong spatial modulation of the photoluminescence emission intensity. The emission intensity at the crest is much higher than the intensity at the trough with a ratio range from 5-7 at the 10% compression. We note that the photoluminescence intensity is highly sensitive to strain, <sup>5,7</sup> doping, <sup>27</sup> and dielectric environment. <sup>28</sup> For example, changing strain in TMDs leads to material dependent changes in the relative band alignment of different optical transitions, <sup>5,7</sup> which in turn leads to material dependent enhancement or suppression of photoluminescence intensity. Additionally, there are contributions to the change in intensity from exciton diffusion, <sup>29</sup> and exciton to trion conversion, <sup>14</sup> though unraveling the relative contributions is beyond the scope of this work.

## 4. MECHANICAL RECONFIGURATION

A major advantage of thin films on soft substrates is that it is easy to vary the magnitude and shape of the wrinkling by tuning the strain of the substrate. In Figure 3, we take advantage of this capability to demonstrate mechanical reconfigurability of the inhomogeneous band structure in the wrinkled WSe<sub>2</sub>. We map the photoluminescence in the same region while varying the uniaxial substrate strain through a range of values  $\epsilon_x = -23.6\%, -14.3\%, -2.6\%, -22.8\%, +15\%, +35.1\%$ , respectively. Figures 3(a-f) show the maps of the photoluminescence transition energy at each respective strain, while Figures 3(g-l) show the corresponding maps of the photoluminescence emission intensity. Here a negative  $\epsilon_x$  indicates compression compared with the initial prestrain while a positive  $\epsilon_x$  indicates tension. Because of the Poisson ratio of the substrate, the perpendicular strain  $\epsilon_y$  also varies, which we confirm by measuring the change in substrate size. However, the edges of the substrate are not clamped, and  $\epsilon_y$  is not independently controlled.

Seen in Figure 3(a,g), at larger substrate compression of -23.6%, there is stronger tuning of the emission energy and intensity along the ripples with  $\Delta E$ =38 meV  $\pm$  5 meV from the crest to the trough. Seen in 3(c,i), as the compression is reduced to near zero, the wavelength of wrinkling increases, and the magnitude of the modulations are significantly reduced. Seen in Figure 3(d,j), when returning to the initial compression near -22.8%, the magnitude and wavelength return to similar values as seen in Figure 3(a,g). Finally, when straining the substrate beyond the initial pre-strain, so the sample is under tension, Figures 3(e-f) show that there is initially a disordered state before ripples emerge along the other direction, corresponding with compression from the Poisson ratio along  $\epsilon_y$ . Finally, we note that the sample shows nearly the same morphology and magnitude of tuning after repeatedly stretching and releasing the substrate 20 times. Importantly, though the substrate strains  $\pm 30\%$  are large compared with the fracture strains of TMDs of 10%, 31 the wrinkling keeps the strains

from building up, and there is no evidence of cracking as a result of the strain cycling of the substrate indicating the viability of this approach to straintronic and wearable devices. We do note that after multiple optical measurements, we observe a change in contrast of the 2D material at the crests of the wrinkles, which we hypothesize is caused by an increased sensitivity to defect creation in the material when under strain. Taken together, these results show that the combination of monolayer 2D material on a wrinkled ALD film has very low interfacial slippage, showing that this is a robust route to mechanically reconfiguring not just the magnitude but the morphology of photonic properties with inhomogeneous strain and strain gradients in 2D materials.

### 5. CONCLUSIONS

In this paper, we demonstrated a simple self-assembly method through wrinkling of 2D monolayers on ALD films to induce periodic modulation of strain and resulting photonic states within the monolayer. Because the ALD film is pre-deposited onto the 2D material, it makes intimate contact with strong adhesion, enabling both the transfer of the 2D material onto the soft substrate and preventing slip or cracking of the 2D material through the large changes in substrate strain. This technique borrows from similar techniques of thin film buckling frequently used in flexible and stretchable electronics. Thus this approach should easily extend to more complex 2D heterostructures and devices, enabling integration of 2D materials into functional device architectures, which has direct applications in stretchable electronics and highly flexible hinges for origami nanostructures. He ven more interesting, integrating strain gradients into device architectures enables access and control of strain dependent quantum states like single quantum emitters, exciton diffusion, and asymmetric valley states. On the strain dependent quantum states like single quantum emitters, exciton diffusion, and asymmetric valley states.

### ACKNOWLEDGMENTS

This research was solely supported by the National Science Foundation MRSEC program under NSF Award Number DMR-1720633. This work was carried out in the Fredrick-Seitz Material Research Laboratory Central Facilities and the Micro and Nano Technology Laboratory, and the iMRSEC shared facilities DMR-1720633. We thank Fubo Rao with assistance in ALD deposition and Siyuan Huang, Hyunchul Kim, Paolo Furlanetto Ferrari, and Pinshane Huang for helpful discussions.

### REFERENCES

- [1] Li, J., Shan, Z., and Ma, E., "Elastic strain engineering for unprecedented materials properties," MRS Bulletin 39(2), 108–114 (2014).
- [2] Del Alamo, J. A., "Nanometre-scale electronics with iii–v compound semiconductors," *Nature* **479**(7373), 317–323 (2011).
- [3] Dai, Z., Liu, L., and Zhang, Z., "Strain engineering of 2d materials: issues and opportunities at the interface," *Advanced Materials* **31**(45), 1805417 (2019).
- [4] Deng, S. and Berry, V., "Wrinkled, rippled and crumpled graphene: an overview of formation mechanism, electronic properties, and applications," *Materials Today* **19**(4), 197–212 (2016).
- [5] Aslan, O. B., Deng, M., and Heinz, T. F., "Strain tuning of excitons in monolayer wse 2," *Physical Review B* 98(11), 115308 (2018).
- [6] He, K., Poole, C., Mak, K. F., and Shan, J., "Experimental demonstration of continuous electronic structure tuning via strain in atomically thin mos2," *Nano letters* **13**(6), 2931–2936 (2013).
- [7] Conley, H. J., Wang, B., Ziegler, J. I., Haglund, R. F., Pantelides, S. T., and Bolotin, K. I., "Bandgap Engineering of Strained Monolayer and Bilayer MoS2," *Nano Letters* **13**, 3626–3630 (aug 2013).
- [8] Feng, J., Qian, X., Huang, C.-W., and Li, J., "Strain-engineered artificial atom as a broad-spectrum solar energy funnel," *Nature Photonics* **6**(12), 866–872 (2012).
- [9] Palacios-Berraquero, C., Kara, D. M., Montblanch, A. R.-P., Barbone, M., Latawiec, P., Yoon, D., Ott, A. K., Loncar, M., Ferrari, A. C., and Atatüre, M., "Large-scale quantum-emitter arrays in atomically thin semiconductors," *Nature communications* 8(1), 1–6 (2017).
- [10] Kumar, S., Kaczmarczyk, A., and Gerardot, B. D., "Strain-induced spatial and spectral isolation of quantum emitters in mono- and bilayer wse2," *Nano Letters* **15**(11), 7567–7573 (2015). PMID: 26480237.

- [11] Rosenberger, M. R., Dass, C. K., Chuang, H.-J., Sivaram, S. V., McCreary, K. M., Hendrickson, J. R., and Jonker, B. T., "Quantum calligraphy: writing single-photon emitters in a two-dimensional materials platform," *ACS nano* 13(1), 904–912 (2019).
- [12] Li, H., Contryman, A. W., Qian, X., Ardakani, S. M., Gong, Y., Wang, X., Weisse, J. M., Lee, C. H., Zhao, J., Ajayan, P. M., Li, J., Manoharan, H. C., and Zheng, X., "Optoelectronic crystal of artificial atoms in strain-textured molybdenum disulphide," *Nature Communications* 6(May) (2015).
- [13] Castellanos-Gomez, A., Roldán, R., Cappelluti, E., Buscema, M., Guinea, F., van der Zant, H. S. J., and Steele, G. A., "Local strain engineering in atomically thin mos2," *Nano Letters* 13(11), 5361–5366 (2013). PMID: 24083520.
- [14] Harats, M. G., Kirchhof, J. N., Qiao, M., Greben, K., and Bolotin, K. I., "Dynamics and efficient conversion of excitons to trions in non-uniformly strained monolayer WS2," *Nature Photonics* **14**(5), 324–329 (2020).
- [15] Cheng, T., Zhang, Y., Lai, W.-Y., and Huang, W., "Stretchable thin-film electrodes for flexible electronics with high deformability and stretchability," *Advanced Materials* **27**(22), 3349–3376 (2015).
- [16] Zang, J., Ryu, S., Pugno, N., Wang, Q., Tu, Q., Buehler, M. J., and Zhao, X., "Multifunctionality and control of the crumpling and unfolding of large-area graphene," *Nature materials* **12**(4), 321–325 (2013).
- [17] Zang, J., Cao, C., Feng, Y., Liu, J., and Zhao, X., "Stretchable and high-performance supercapacitors with crumpled graphene papers," *Scientific reports* 4(1), 1–7 (2014).
- [18] Yu, J., Kim, S., Ertekin, E., and van der Zande, A. M., "Material-dependent evolution of mechanical folding instabilities in two-dimensional atomic membranes," *ACS Applied Materials & Interfaces* **12**(9), 10801–10808 (2020). PMID: 32036649.
- [19] Lee, W.-K., Kang, J., Chen, K.-S., Engel, C. J., Jung, W.-B., Rhee, D., Hersam, M. C., and Odom, T. W., "Multiscale, hierarchical patterning of graphene by conformal wrinkling," *Nano Letters* **16**(11), 7121–7127 (2016). PMID: 27726404.
- [20] Rhee, D., Paci, J. T., Deng, S., Lee, W.-K., Schatz, G. C., and Odom, T. W., "Soft Skin Layers Enable Area-Specific, Multiscale Graphene Wrinkles with Switchable Orientations," ACS Nano 14, 166–174 (jan 2020).
- [21] Han, E., Yu, J., Annevelink, E., Son, J., Kang, D. A., Watanabe, K., Taniguchi, T., Ertekin, E., Huang, P. Y., and van der Zande, A. M., "Ultrasoft slip-mediated bending in few-layer graphene," *Nature Materials* 19(3), 305–309 (2020).
- [22] Hu, K.-M., Liu, Y.-Q., Zhou, L.-W., Xue, Z.-Y., Peng, B., Yan, H., Di, Z.-F., Jiang, X.-S., Meng, G., and Zhang, W.-M., "Delamination-free functional graphene surface by multiscale, conformal wrinkling," *Advanced Functional Materials* n/a(n/a), 2003273.
- [23] Liu, F., Wu, W., Bai, Y., Chae, S. H., Li, Q., Wang, J., Hone, J., and Zhu, X. Y., "Disassembling 2D van der Waals crystals into macroscopic monolayers and reassembling into artificial lattices," *Science* **367**(6480), 903–906 (2020).
- [24] Gurarslan, A., Yu, Y., Su, L., Yu, Y., Suarez, F., Yao, S., Zhu, Y., Ozturk, M., Zhang, Y., and Cao, L., "Surface-energy-assisted perfect transfer of centimeter-scale monolayer and few-layer mos2 films onto arbitrary substrates," ACS nano 8(11), 11522–11528 (2014).
- [25] Wang, Q. and Zhao, X., "A three-dimensional phase diagram of growth-induced surface instabilities," Scientific Reports 5(1), 8887 (2015).
- [26] Mills, A., Yu, Y., Chen, C., Huang, B., Cao, L., and Tao, C., "Ripples near edge terminals in mos2 few layers and pyramid nanostructures," Applied Physics Letters 108(8), 081601 (2016).
- [27] Chernikov, A., van der Zande, A. M., Hill, H. M., Rigosi, A. F., Velauthapillai, A., Hone, J., and Heinz, T. F., "Electrical tuning of exciton binding energies in monolayer ws2," Phys. Rev. Lett. 115, 126802 (Sep 2015).
- [28] Raja, A., Chaves, A., Yu, J., Arefe, G., Hill, H. M., Rigosi, A. F., Berkelbach, T. C., Nagler, P., Schüller, C., Korn, T., Nuckolls, C., Hone, J., Brus, L. E., Heinz, T. F., Reichman, D. R., and Chernikov, A., "Coulomb engineering of the bandgap and excitons in two-dimensional materials," *Nature Communications* 8(1), 15251 (2017).

- [29] Hotta, T., Higuchi, S., Uchiyama, Y., Ueno, K., Watanabe, K., Taniguchi, T., Shinohara, H., and Kitaura, R., "Exciton diffusion in hbn-encapsulated monolayer mose2," in [2019 Compound Semiconductor Week (CSW)], 1–2 (2019).
- [30] Wang, B., Bao, S., Vinnikova, S., Ghanta, P., and Wang, S., "Buckling analysis in stretchable electronics," npj Flexible Electronics 1(1), 5 (2017).
- [31] Bertolazzi, S., Brivio, J., and Kis, A., "Stretching and breaking of ultrathin mos2," *ACS Nano* **5**(12), 9703–9709 (2011). PMID: 22087740.
- [32] Khang, D.-Y., Rogers, J. A., and Lee, H. H., "Mechanical buckling: Mechanics, metrology, and stretchable electronics," *Advanced Functional Materials* **19**(10), 1526–1536 (2009).
- [33] Xue, Z., Song, H., Rogers, J. A., Zhang, Y., and Huang, Y., "Mechanically-guided structural designs in stretchable inorganic electronics," *Advanced Materials* **32**(15), 1902254 (2020).
- [34] Lim, S., Luan, H., Zhao, S., Lee, Y., Zhang, Y., Huang, Y., Rogers, J. A., and Ahn, J.-H., "Assembly of foldable 3d microstructures using graphene hinges," *Advanced Materials* **32**(28), 2001303 (2020).
- [35] Miskin, M. Z., Dorsey, K. J., Bircan, B., Han, Y., Muller, D. A., McEuen, P. L., and Cohen, I., "Graphene-based bimorphs for micron-sized, autonomous origami machines," *Proceedings of the National Academy of Sciences* 115(3), 466–470 (2018).
- [36] Cordovilla Leon, D. F., Li, Z., Jang, S. W., Cheng, C.-H., and Deotare, P. B., "Exciton transport in strained monolayer wse2," *Applied Physics Letters* **113**(25), 252101 (2018).
- [37] Jena, N., Dimple, Ahammed, R., Rawat, A., Mohanta, M. K., and De Sarkar, A., "Valley drift and valley current modulation in strained monolayer Mos<sub>2</sub>," *Phys. Rev. B* **100**, 165413 (Oct 2019).